Geoderma xxx (xxxx) xxx–xxx

Contents lists available at ScienceDirect

Geoderma

journal homepage: www.elsevier.com/locate/geoderma

Understanding the fate of soil organic matter in submerging coastal wetland soils: A microcosm approach

Havalend E. Steinmuller[a], Kyle M. Dittmer[a,b], John R. White[c], Lisa G. Chambers[a,*]

[a] Aquatic Biogeochemistry Laboratory, Department of Biology, University of Central Florida, Orlando, FL 32816, United States of America
[b] Global Change Biogeochemistry Laboratory, Rubenstein School of Environment and Natural Resources, University of Vermont, Burlington, VT 05405, United States of America
[c] Wetland and Aquatic Biogeochemistry Laboratory, Department of Oceanography and Coastal Sciences, Louisiana State University, Baton Rouge, LA 70803, United States of America

ARTICLE INFO

Keywords:
Sea level rise
Wetland submergence
Soil organic matter
Carbon dioxide production
Blue carbon

ABSTRACT

Coastal wetland submergence can occur when rates of relative sea-level rise exceed that of soil elevation gain or landward transgression. In highly organic soils, the collapse of the wetland platform into open water can cause disarticulation of the soil structure, exposing previously protected anaerobic microzones to oxygenated seawater, which may accelerate mineralization rates. Nine soil cores (1 m deep) were collected from three sites within Barataria Bay, LA (USA), a region known for high rates of wetland submergence. Both the biogeochemical properties of the soils with depth were determined, as well as the impacts of the introduction of oxygenated seawater on carbon mineralization rates. Both field enzyme activity (β-glucosidase, *N*-acetyl-beta-D-glucosaminidase, alkaline phosphatase, β-xylosidase, and β-cellobiosidase) and microbial biomass carbon (MBC) did not significantly change with depth until 50 cm, where activity increased dramatically, then gradually decreased. Total carbon (C), total nitrogen, and percent organic matter were highest between 50 and 100 cm. Following initial biogeochemical characterization, soil microcosms were created for 11 depth segments under anaerobic conditions (mimicking an intact wetland) and aerobic conditions (mimicking a submerging wetland mixing with oxygenated water); carbon dioxide (CO_2) production was measured within the bottles over 14 days. Carbon dioxide production averaged 66% greater in the aerobic treatment than the anaerobic treatment. Both treatments exhibited a general trend of increasing CO_2 production with depth (particularly from 40 to 100 cm), with the difference in CO_2 production between aerobic and anaerobic treatments being 4× greater at 90–100 cm than at the soil surface (0–5 cm). The increase in C mineralization rates observed at depth was positively correlated with indicators of greater microbial activity (i.e., higher enzyme activity and MBC) and greater nutrient availability. Study results indicate coastal wetland submergence into open water could significantly enhance CO_2 emissions, even in deep (40 + cm) soils, contrary to the typically observed pattern of soil microbial activity and soil quality decreasing with depth. These findings underline the need to analyze deeper soil samples (1 + m) in order to fully understand the implications of sea level rise on C loss from submerging coastal wetland soils.

1. Introduction

Coastal wetlands rank as one of the most productive ecosystem types on Earth (Amthor and Huston, 1998). High rates of primary production coupled with prevailing anaerobic conditions from tidal flooding allow salt marsh sediments to sequester 244.7 $g\,C\,m^{-2}\,y^{-1}$ (Ouyang and Lee, 2014). Wetland macrophytes contain different forms of organic compounds that are deposited on the soil surface as detritus when plants senesce. These materials can contain recalcitrant lignins and tannins, but also include significant quantities of labile, low molecular weight compounds that are rapidly and preferentially degraded by microbial consortia in the surficial soil (Reddy and DeLaune, 2008; Bianchi and Canuel, 2011). The remaining recalcitrant, high molecular weight organic compounds are subsequently buried and comprise the extensive peat deposits found within many coastal wetlands (DeBusk and Reddy, 1998). These processes are the foundation of a 'decay continuum', where soil organic carbon (C) gradually becomes more refractory and recalcitrant over time (Melillo et al., 1989). Additionally,

* Corresponding author.
E-mail address: lisa.chambers@ucf.edu (L.G. Chambers).

https://doi.org/10.1016/j.geoderma.2018.08.020
Received 31 December 2017; Received in revised form 31 July 2018; Accepted 16 August 2018

it is generally accepted that microbial processes such as decomposition decrease with depth, due to prevailing anaerobic conditions and a decrease in both the availability of labile organic compounds and electron acceptors (Gale and Gilmour, 1988; Maltby, 1988; Mendelssohn et al., 1999; Schipper and Reddy, 1995; Schipper et al., 2002; Webster and Benfield, 1986). High organic C accumulation rates within coastal wetlands are facilitated by the burial of organic matter throughout the 'decay continuum'. For example, in coastal Louisiana salt marshes, organic C accumulation ranges from 132 g m^{-2} yr^{-1} (DeLaune and Pezeshki, 2003) to 310 g m^{-2} yr^{-1} (Hatton et al., 1983). Combined with vertical accretion rates of 0.75–1.35 cm yr^{-1} (Delaune et al., 1981), projected annual C accumulation in these wetlands is roughly 30 kg C m^{-2} (DeLaune and White, 2012). However, these vast pools of soil organic C, and the associated nutrients found within organic matter, may be threatened by rising sea levels.

The eustatic sea level rise rate is currently 3.4 ± 0.4 mm yr^{-1} and is expected to continue rising throughout the next century (IPCC, 2014). Coastal wetlands, which form the interface between terrestrial and marine systems, are particularly vulnerable to sea level rise. In response to the combined stressors of increased inundation and salinity, coastal wetlands respond to sea level rise in three distinct patterns: (a) by maintaining their position within the coastal landscape by accreting vertically at a rate that either matches or exceeds sea level rise, (b) transgressing landward to occupy a more conducive elevation within the coastal plain, or (c) submerging, which occurs when relative sea level rise rates exceed rates of soil surface elevation gain (Kirwan and Megonigal, 2013).

Coastal wetlands within Barataria Bay, Louisiana, USA are responding to increases in sea level predominantly via submergence, and the subsequent complete conversion of previously wetland habitat to open water (Baumann et al., 1984). Relative sea level rise rates in Barataria Bay rank among the highest in the world, averaging ~13 mm y^{-1} (Church et al., 2013). The combination of subsidence via tectonic downwarping, eustatic sea level rise, erosive processes (as high as 3–5.5 mm d^{-1} in some places, J.R. White, unpublished data), and a lack of sediment inputs, have resulted in Barataria Bay losing approximately 25.9 km^2 yr^{-1} (Penland et al., 2000). As these wetlands are lost, 1 to 2 m of accumulated organic-rich soil also submerges (DeLaune and White, 2012). Vegetation death and wetland submergence result in a loss of soil structure, and the wetland platform collapses (DeLaune and White, 2012).

Following submergence, the accumulated soil organic matter can be either reburied within the bay or mineralized in the water column, being released as CO_2 into the atmosphere or as dissolved inorganic C within the water column. During the mineralization process, stored nutrients within the soil organic matter, such as nitrogen (N) and phosphorus (P), can also be released into the coastal zone (Bianchi et al., 2008). The high bulk density and low organic matter content of bay sediments suggest that coastal peat deposits are not reburied within the bay (Pietroski et al., 2015; White et al., 2009). Rather, as sequestered wetland soil organic materials are submerged and disarticulated in a more turbulent open water environment, the previously protected anaerobic microzones within the soil are exposed to oxygenated seawater. Under these conditions, microbial respiration is expected to increase, owing to oxygen being the most efficient and thermodynamically favored respiration pathway (Reddy and DeLaune, 2008). The addition of oxygen as an electron acceptor has been shown to catalyze increases in the mineralization of organic matter, concomitantly increasing concentrations of inorganic N and P (Bridgham et al., 1998; McLatchey and Reddy, 1998; Updegraff et al., 1995). Decomposition of organic material and the release of N and P into the water column could potentially exacerbate nutrient pollution present in deltaic Louisiana and contribute to hypoxic events (Eldridge and Morse, 2008; Bianchi et al., 2008). While studies have acknowledged the importance of inputs of terrestrial organic matter to the coastal zone (Odum, 1968), the magnitude of inputs via coastal wetland submergence has not been well studied. This study aims to understand the fate of soil organic matter, particularly C, N, and P, following sea level-rise induced coastal wetland submergence. Specifically, the potential mineralization of organic coastal wetland soils with depth under anaerobic conditions (to mimic decomposition rates within an intact marsh), and aerobic conditions (to mimic decomposition rates within a submerging marsh subjected to oxygen-rich seawater) were investigated. We hypothesized that the exposure to oxygen-rich seawater would result in an increase in mineralization potential, concomitant with increases in other indicators of microbial biomass and activity. We expected that these changes would be mediated by depth, with the magnitude of the increase in CO_2 production due to oxygenation decreasing with depth due to the changing ratio of labile: recalcitrant C.

2. Methods

2.1. Study area

Barataria Bay, a 6333 km^2 area of shallow open water and coastal wetlands, is located immediately west of the Mississippi River delta and east of Bayou Lafourche in southeastern Louisiana (USA). Salinity concentrations in the salt marsh zone within the bay range from 6 to 22 ppt, depending on season, location, freshwater input, tidal flux, and prevailing winds (Levine et al., 2017; Rakocinski et al., 1992). Tides within the bay are generally diurnal, and average 0.3 m (Conner and Day, 1987). At the time of sampling, percent dissolved oxygen was between 79 and 108% saturation at 1 m depth in the water column within the bay, and averaged ~8 mg/L from March to May of 2017 (USGS Monitoring Station #07380251; U.S. Geological Survey, 2018), representing a well oxygenated system. Hydrologic flux within the bay is dominated by tidal flushing, storm events, and wind-driven circulation, contributing to relatively high dissolved oxygen concentrations within the bay (Conner and Day, 1987). Three marshes were selected for sampling (Fig. 1), based on similar hydrologic regimes, ecogeomorphic characteristics, and vegetation communities (i.e., all sites were dominated by *Spartina alterniflora*).

2.2. Soil and water sampling

All three sites were sampled ~2 weeks apart throughout early spring of 2017. At each of the three sites, one (1) liter of surface water was collected ~10 cm below the water surface. Three (3) soil cores were taken via the push-core method to a depth of 100 cm at each site, 1 m from the coastal edge, within the marsh platform. Each of the nine (9) cores were extruded into 11 depth segments: 0–5, 5–10, 10–20, …, 90–100 cm. Soil samples were placed in sealed polyethylene bags and placed on ice, then immediately transported to the laboratory. Soil and water samples were kept at 4 °C until being shipped overnight, on ice, to University of Central Florida for analysis. Site water was filtered through Supor 0.45 μM filters upon arrival.

2.3. Soil physiochemical properties

Soil bulk density and moisture content were determined by drying a subsample of soil using a gravimetric oven at 70 °C after 3 days or until a constant weight was achieved. Dried soils were ground using a SPEX Sample Prep 8000M Mixer/Mill (Metuchen, NJ). Dried, ground subsamples were used to determine percent organic matter using the loss-on-ignition method, where soils were burned at 550 °C in a muffle furnace for a total of 3 h. Following determination of percent organic matter, soils were digested with 50 mL of 1 N HCl at 100 °C for 30 min, then filtered through Whatman #41 filter paper for total P analysis (Andersen, 1976). Total P content was then determined colorimetrically via an AQ2 Automated Discrete Analyzer (Seal Analytical, Mequon, WI) in accordance with EPA method 365.1 Rev. 2. Total C and N content was determined by use of a Vario Micro Cube CHNS Analyzer

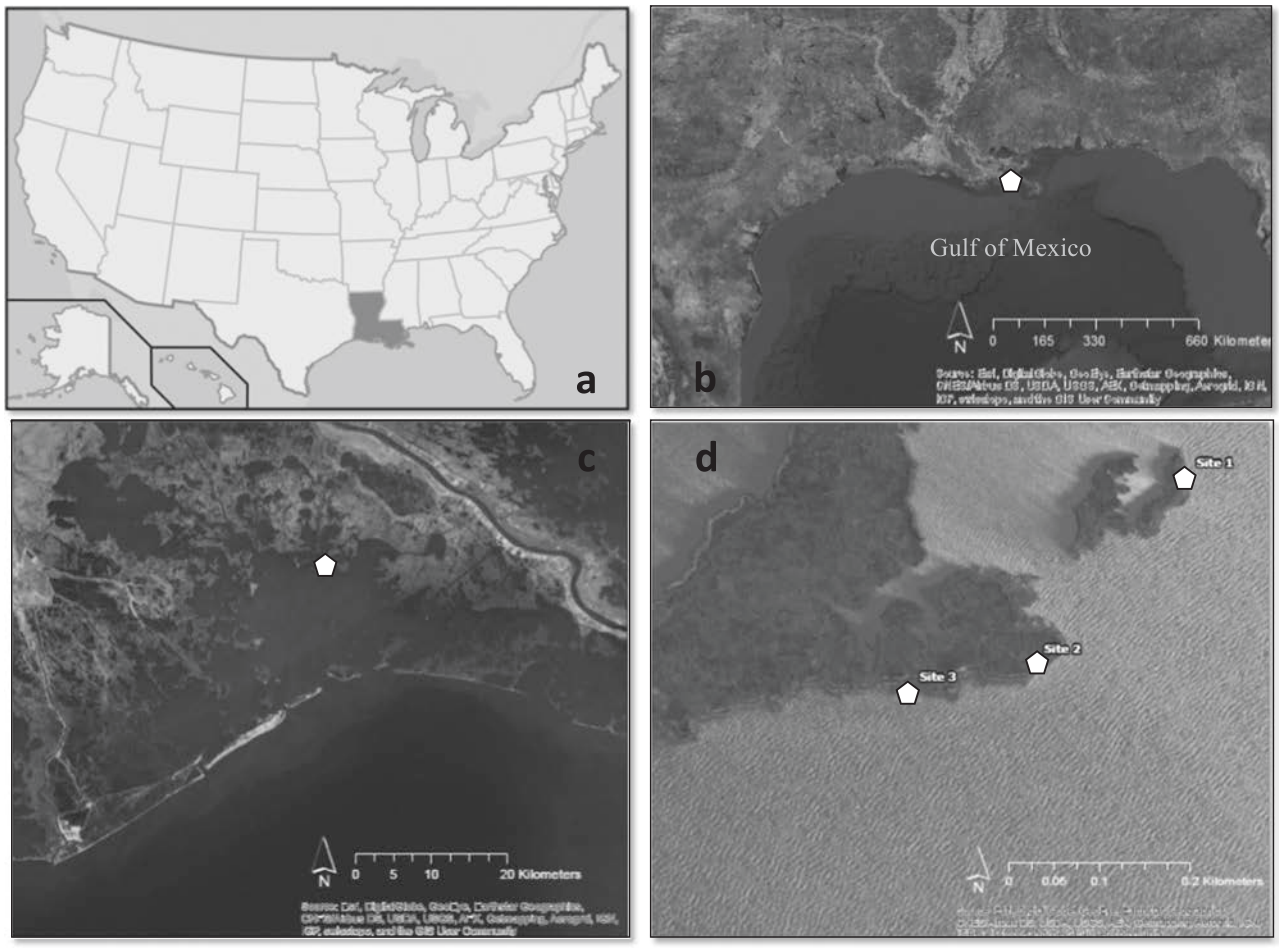

Fig. 1. Map of site location. All sites are located within Barataria Bay, LA.

(Elementar Americas Inc., Mount Laurel, NJ). Soil pH was determined by creating a 1:5 slurry of soil to distilled, deionized water, and subsequent measurement using an Accument bench top pH probe (Accumet XL200, ThermoFisher Scientific, Waltham, MA, USA).

2.4. Greenhouse gas production

Soils were homogenized and duplicate subsamples (approximately 7 g) from each depth segment of each core were weighed into 100 mL glass serum bottles. All bottles were capped with a rubber septa and aluminum crimp and evacuated to −75 mm Hg. Replicate bottles were randomly assigned to one of two treatments: anaerobic (purged with 99% O_2-free N_2 gas for 3 min), or aerobic (purged with Breathing Grade air containing 21% O_2 for 3 min). Anaerobic bottles were injected with 14 mL of filtered, N_2-purged site water, while aerobic bottles were injected with 14 mL of filtered, breathing air-purged site water. Bottles were then placed on an orbital shaker at 150 rpm and 25 °C. Headspace samples were taken at 1, 2, 4, 7, 10, and 14 day time points, and injected into a GC-2014 gas chromatograph (Shimadzu Instrument, Kyoto, Japan) equipped with a flame ionization detector. Respiration rates were calculated as the change in CO_2 production over time. After each gas sample was extracted from the bottles' headspace, the bottle was purged with either 99% O_2-free N_2 gas or Breathing Grade air for 3 min, depending on treatment. Additionally, methane (CH_4) production was analyzed on the same instrument at the same time. However, CH_4 production was generally below detection, and thus results are not discussed.

Following the 14 day incubation, bottles were uncapped, and the remaining soil sample was placed in a 20 mL HDPE scintillation vials for analysis of extractable ammonium (NH_4^+), nitrate (NO_3^-), and soluble reactive phosphorus (SRP), microbial biomass C, and enzyme analysis.

2.5. Extractable nutrient analysis

Extractable nutrient analyses (DOC, NH_4^+, NO_3^-, and SRP) occurred on soils immediately after field sampling (time zero), and on soils from the bottles after the 14-day incubation. Rates of potentially mineralizable nutrients were calculated as the extractable nutrient concentration after the 14-day incubation minus the initial extractable nutrient concentration, divided by the 14 days. The extraction process consisted of weighing 2.5 g of wet soil (both from the field and from the bottle incubation) into 40 mL centrifuge tubes and adding 25 mL of 2 M KCl. Samples were then shaken continuously on an orbital shaker for 1 h at 25 °C and 150 rpm, then centrifuged for 10 min at 10 °C and 5000 rpm. Following the centrifuge, samples were immediately filtered through Supor 0.45 μM filters and acidified with double distilled H_2SO_4 to a pH of < 2 for preservation. Extractable nutrients samples were then analyzed using an AQ2 Automated Discrete Analyzer (Seal Analytical, Mequon, WI, EPA methods 231-A Rev.0, 210-A Rev.1, and 204-A Rev.0).

2.6. Microbial biomass carbon

Microbial biomass C (MBC) was determined on soils both immediately after the field sampling and soils from the bottles after the incubation period following the method outlined in Vance et al. (1987). Duplicates of approximately 1 g dry weight of field-moist soil were

weighed into 40 mL centrifuge tubes and assigned to either a fumigate or non-fumigate treatment. The fumigated samples were exposed to gaseous chloroform for 24 h in a glass desiccator. After 24 h, the samples were extracted with 25 mL of 0.5 M K_2SO_4, placed in an orbital shaker for 1 h at 25 °C and 150 rpm. After incubation, samples were immediately centrifuged for 10 min at 10 °C and 5000 rpm. The supernatant was vacuum filtered through Supor 0.45 μM filters, acidified with double distilled H_2SO_4 for preservation, and stored at 4 °C until analysis. Non-fumigate samples were processed in the same manner, excluding the chloroform fumigation. Dissolved organic carbon (DOC) was determined by use of a Shimadzu TOC-L Analyzer (Kyoto, Japan). Microbial biomass C was calculated as the difference between the fumigated samples and the non-fumigated samples.

2.7. Enzyme activity

Extracellular enzyme assays were performed to determine activity of β-glucosidase (BG), *N*-acetyl-beta-D-glucosaminidase (NAG), alkaline phosphatase (AP), β-xylosidase (XY), and β-cellobiosidase (CB). Similar to extractable nutrients and microbial biomass C, extracellular enzyme assays were performed on both initial soil samples after they were retrieved from the field, and soils following the bottle incubation. Assays were conducted using fluorescent substrate 4-methylumbelliferone (MUF) for standardization and fluorescently labeled MUF-specific substrates (German et al., 2011). To create a 1:100 slurry, 0.5 g of soil was added to 39 mL of autoclaved distilled deionized water and shaken continuously on an orbital shaker for 1 h at 25 °C and 150 rpm. Fluorescence was measured at excitation/emission wavelengths 360/460 on a BioTek Synergy HTX (BioTek Instruments, Inc., Winooski, VT, USA) both immediately after substrate and sample were added, and 24 h later to determine a rate of enzyme activity.

2.8. Statistical analysis

All statistical analysis was performed using R (R Foundation for Statistical Computing, Vienna, Austria) within RStudio (RStudio Team, 2015). Prior to determining significance, all parameters were analyzed for homogeneity of variance using Levene's test, and assumptions of normality using the Shapiro-Wilk test. If datasets were not normal, they were transformed using a logarithmic transformation to meet the assumptions of normality.

Data was separated into field characteristics (before the incubation), and experimental results (following the incubation). Field characteristics were analyzed using a linear mixed-effect model in R with site and depth as predictor variables. 'Core' was included as a random effect to test for effects of replicate cores taken at each site. Post-hoc tests were conducted using package lsmeans via the Tukey method. Pearson product-moment correlations were also performed between all field characteristics. Significance was determined based on an alpha value of 0.05 for all tests, and adjusted with a Bonferroni correction to 0.004.

Experimental results were analyzed via a linear mixed-effect model in R with treatment, depth, the interaction between treatment and depth, and site as predictor variables. Core was again included as a random effect. The lsmeans package was used to determine post-hoc significance based on the Tukey method. Significance was determined based on an alpha value modified by a Bonferroni correction to 0.004.

3. Results

3.1. Field characteristics

3.1.1. Physiochemical data

Moisture content changed significantly with depth, ranging from 63.5 ± 2.0% at the surface (0–5 cm) to 85.5 ± 0.5% at 70–80 cm and generally increasing with depth (Table 1). Moisture content was negatively correlated to bulk density, and strongly positively correlated to organic matter content, total N, total C, and extractable NO_3^- (Table 2). Moisture content was weakly correlated to NAG, AP, BG, and XY activity (Table 2). Depth was also a significant predictor variable for bulk density, ranging from 0.21 ± 0.2 g cm^{-3} at 20–30 cm to 0.07 ± 0.1 g cm^{-3} at 70–80 cm (Table 1). Organic matter content, total C and total N were all correlated to each other, and with depth (Table 1, Table 2). Within the 0–50 cm depth intervals, organic matter content averaged 19.1 ± 0.74% (Fig. 2). Deeper than 50 cm, organic matter content averaged 43.9 ± 2.3%. Total N displayed the same trend, with lower values in the top 50 cm (4.41 ± 0.22 g kg^{-1}), and higher values in the bottom 50 cm (11.1 ± 0.59 g kg^{-1}). Similarly, total C averaged 85.0 ± 3.9 g kg^{-1} in the upper 50 cm and 220.5 ± 11.4 g kg^{-1} in the lower 50 cm. Both total C and N were significantly correlated to NAG, AP, BG, and XY activity, as well as extractable NO_3^- (Table 2). Total P was not significant with depth (Table 1). Also, site was not a significant predictor variable for any physiochemical measurement (Table 3).

3.1.2. Enzyme activity

Site was a significant predictor variable for all measured enzyme activities (Table 1). *N*-acetyl-beta-D-glucosaminidase activity ranged from 17.7 ± 1.60 nmol MUF g^{-1} min^{-1} at site 2, and 3.18 ± 0.54 nmol MUF g^{-1} min^{-1} at site 1. The lowest enzyme activity was consistently measured within site 1. Alkaline phosphatase activity at site 1 was 2.94 ± 0.32 nmol MUF g^{-1} min^{-1}. Comparatively, XY activity was 1.69 ± 0.15 nmol MUF g^{-1} min^{-1} and CB activity was 1.54 ± 0.25 nmol MUF g^{-1} min^{-1}. The greatest AP activity was within site 3, where activity was 19.6 ± 4.64 nmol MUF g^{-1} min^{-1}. CB and XY activity were greatest within site 2. β-Glucosidase activity was

Table 1
p-Values associated with each parameter tested using linear model. α = 0.004. Values in bold denote significance. Ext. refers to 'extractable'.

Field characteristics

	% OM	Total C	Total N	Total P	NAG	AP	BG	XY	CB	Ext. DOC	Ext. NO_3^-	Ext. NH_4^+	MBC
Site	0.5426	0.6638	0.0876	**0.0276**	< **0.0001**	**0.0001**	**0.0001**	< **0.0001**	< **0.0001**	0.9679	0.5252	0.6327	0.006
Depth	< **0.0001**	< **0.0001**	< **0.0001**	0.0966	< **0.0001**	0.0131	0.0301	**0.0026**	0.2084	**0.0001**	< **0.0001**	< **0.0001**	< **0.0001**

Experimental results

	NAG	AP	BG	XY	CB	MBC	CO_2 production	PMN
Treatment	**0.0025**	0.5799	0.1494	0.0565	0.2387	0.4851	**0.0003**	**0.0001**
Depth	< **0.0001**	< **0.0001**	< **0.0001**	**0.0029**	**0.0017**	< **0.0001**	< **0.0001**	0.0205
Site	0.6569	0.9153	< **0.0001**	< **0.0001**	< **0.0001**	**0.0001**	< **0.0001**	< **0.0001**
Treatment * Depth	0.361	0.2974	0.285	0.8464	0.8674	0.5585	0.9245	< **0.0001**

Table 2
Correlation matrix including Pearson product-moment correlations between field characteristics. Degrees of freedom = 99. α = 0.05. Critical value = 0.197. Values in bold are significant, while values that are bold and underlined denote strong significance (critical value > 0.8). Ext. refers to 'extractable'.

	Moisture content	Bulk density	pH	%OM	TC	TN	TP	NAG	AP	BG	XY	CB	Ext. DOC	Ext. NO_3^-	Ext. NH_4^+	Ext. SRP
Bulk density	**−0.85**															
pH	**0.26**	**−0.27**														
%OM	**0.90**	**−0.81**	**0.27**													
TC	**0.91**	**−0.82**	**0.29**	**0.98**												
TN	**0.90**	**−0.84**	**0.33**	**0.96**	**0.98**											
TP	0.05	−0.05	**−0.42**	0.05	0.07	0.05										
NAG	**0.36**	**−0.34**	0.14	**0.49**	**0.47**	**0.42**	0.19									
AP	**0.34**	**−0.32**	0.14	**0.40**	**0.41**	**0.45**	0.17	**0.52**								
BG	**0.30**	**−0.27**	0.07	**0.39**	**0.36**	**0.33**	0.19	**0.69**	**0.27**							
XY	**0.44**	**−0.36**	0.10	**0.53**	**0.51**	**0.46**	0.11	**0.75**	**0.36**	**0.69**						
CB	0.19	−0.13	−0.16	**0.25**	**0.22**	0.18	**0.27**	**0.57**	**0.20**	**0.62**	**0.83**					
Ext. DOC	**0.53**	**−0.45**	0.13	**0.52**	**0.54**	**0.53**	0.02	**0.23**	**0.26**	**0.23**	**0.25**	0.08				
Ext. NO_3^-	**0.81**	**−0.70**	**0.29**	**0.82**	**0.83**	**0.84**	0.08	**0.30**	**0.29**	0.19	**0.24**	0.01	**0.39**			
Ext. NH_4^+	−0.15	−0.01	0.13	−0.10	−0.09	−0.10	0.00	−0.10	−0.08	−0.12	−0.09	−0.03	−0.11	−0.13		
Ext. SRP	0.15	−0.09	−0.03	0.15	0.16	0.19	0.05	0.01	0.09	0.03	−0.01	−0.06	0.04	**0.23**	−0.18	
Microbial C	**0.81**	**−0.72**	**0.29**	**0.84**	**0.85**	**0.87**	0.13	**0.44**	**0.47**	**0.41**	**0.44**	**0.20**	**0.52**	**0.76**	−0.12	0.17

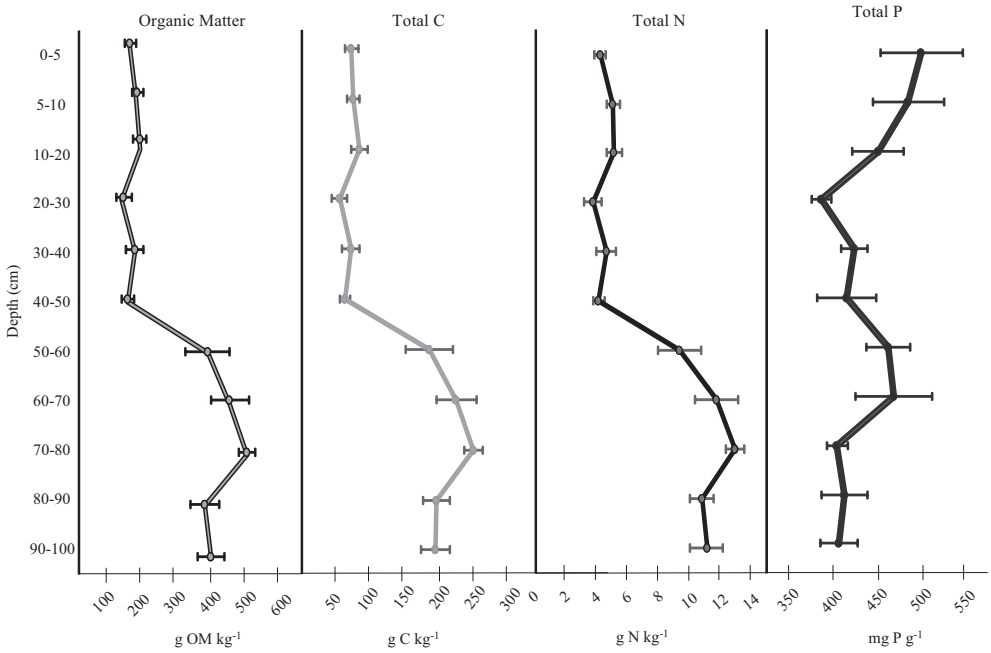

Fig. 2. Organic matter, total C, total N, and total P concentrations in soil with depth. Values shown are mean ± standard error (n = 9).

lowest within site 1, at 4.98 ± 0.48 nmol MUF g^{-1} min^{-1}, and greatest within site 2, at 22.61 ± 1.98 nmol MUF g^{-1} min^{-1}.

Additionally, soil depth affected all enzymes except for CB (Table 1). All enzymes showed a similar trend with depth (Fig. 3). Within the top 50 cm, activity generally decreased from the surface. However, at 50–60 cm, activity increased approximately 50% compared to the 0–5 cm depth interval, then gradually decreased. *N*-acetyl-beta-D-glucosaminidase activity ranged from 5.69 ± 1.91 nmol MUF g^{-1} min^{-1} at 90–100 cm to 29.2 ± 7.81 nmol MUF g^{-1} min^{-1} at 50–60 cm. Alkaline phosphatase activity was lowest at the 90–100 cm depth, where activity was 6.85 ± 1.66 nmol MUF g^{-1} min^{-1}, and greatest within the 60–70 cm depth interval, where activity was 27.2 ± 13.9 nmol MUF g^{-1} min^{-1}. Activity of BG ranged from 5.22 ± 1.14 nmol MUF g^{-1} min^{-1} at 90–100 cm to 32.6 ± 13.6 nmol MUF g^{-1} min^{-1} at 50–60 cm. Xylosidase activity at the 90–100 cm depth was lowest, at 2.83 ± 0.84 nmol MUF g^{-1} min^{-1}, while the 50–60 cm depth was highest, at 8.30 ± 2.97 nmol MUF g^{-1} min^{-1}. Microbial biomass C strongly correlated with all enzyme activity (Table 2). Additionally, NAG, AP, and XY

Table 3
Soil physiochemical parameters by site (averaged over depth intervals) ± standard error (n = 33). Site was not a significant predictor variable for any soil physiochemical parameters.

Site	Moisture content	Bulk density (g cm^{-3})	pH	% Organic Matter	Total C (g kg^{-1})	Total N (g kg^{-1})	Total P (g kg^{-1})
1	0.74 ± 0.01	0.14 ± 0.01	7.10 ± 0.11	28.06 ± 2.17	135.12 ± 11.43	6.55 ± 0.52	429.75 ± 11.86
2	0.75 ± 0.02	0.14 ± 0.01	7.10 ± 0.11	32.24 ± 2.86	152.51 ± 15.74	7.62 ± 0.72	478.48 ± 23.75
3	0.73 ± 0.02	0.13 ± 0.01	7.68 ± 0.05	30.77 ± 3.40	152.16 ± 18.02	8.14 ± 0.91	430.92 ± 9.53

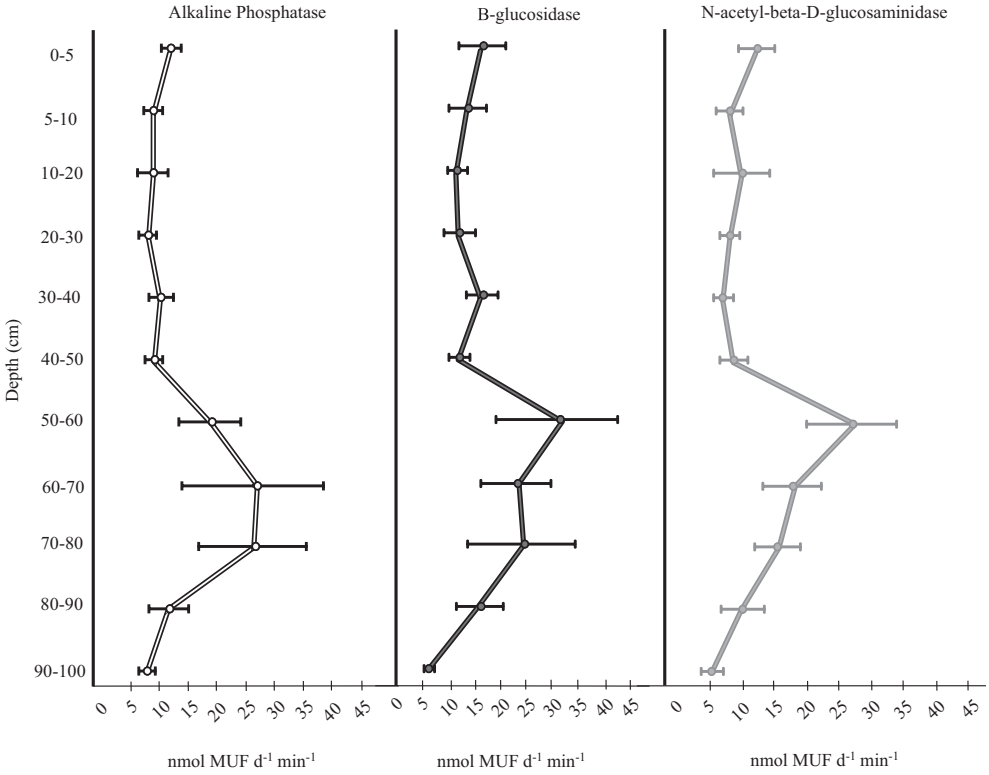

Fig. 3. Initial (field) AP activity, BG activity, and NAG activity with depth. Values shown are mean ± standard error (n = 9).

activity significantly correlated to extractable NO_3^- (Table 2). All enzyme activities were significantly correlated to each other (Table 2).

3.1.3. Microbial biomass C

Microbial biomass C was significantly affected by both site and depth (Table 1). The highest MBC concentrations were found at site 3, with 5904 ± 630 mg kg^{-1}, and lowest at site 1, with 4225 ± 279 mg kg^{-1}. In terms of depth, MBC was generally similar from 0–5 cm to 40–50 cm, averaging 3504 ± 207 mg kg^{-1} (Fig. 4). Below 50 cm, MBC averaged 7377 ± 393 mg kg^{-1}. Microbial biomass C was significantly correlated to both extractable NO_3^- and extractable NH_4^+ concentrations (Table 2).

3.1.4. Extractable nutrients and DOC

Extractable NO_3^- displayed a similar trend to the enzyme activity and MBC data-concentrations were lowest between 0–5 cm and 40–50 cm, then increased below 50 cm (Fig. 5). The lowest extractable NO_3^- concentrations were found at 40–50 cm, 1.61 ± 0.19 mg kg^{-1}, while the highest concentrations were 5.38 ± 0.17 mg kg^{-1} at the 70–80 cm depth. Though depth significantly affected extractable NO_3^-values, site was insignificant (Table 1). Extractable NH_4^+ was significant with depth (Table 1), ranging from 22.6 ± 7.89 mg kg^{-1} at the surface to 1.94 ± 0.30 mg kg^{-1} at 30–40 cm. Extractable DOC was significantly affected by depth (Table 1), and ranged from 163 ± 13.5 mg kg^{-1} at 0–5 cm to 608 ± 52.5 mg kg^{-1} at 60–70 cm. Extractable DOC exhibited a similar trend to extractable NO_3^-, enzyme activity, and MBC. Extractable SRP was consistently below detection (data not shown).

3.2. Experimental results

3.2.1. Carbon dioxide production

Treatment and depth were both significant predictor variables for CO_2 production (Table 1). The anaerobic treatment was consistently lower than the aerobic treatment. To account for the effects of the bottle incubation, the difference in CO_2 production between the aerobic and anaerobic treatment was calculated. In general, the difference in CO_2 production between the two treatments increased with depth, ranging from 0.69 ± 0.20 mg CO_2-C kg^{-1} h^{-1} within the 10–20 cm depth interval to 9.06 ± 0.97 mg CO_2-C kg^{-1} h^{-1} within the 90–100 cm depth interval (Fig. 6).

3.2.2. Enzyme activity

Treatment did not significantly affect any enzyme activity except for NAG (Table 1). *N*-acetyl-beta-D-glucosaminidase activity was significantly higher in the anaerobic treatment, 29.9 ± 2.47 nmol MUF g^{-1} min^{-1}, than the aerobic treatment, 21.2 ± 1.84 nmol MUF g^{-1} min^{-1}. Following the incubation, depth still significantly affected all enzyme activities (Table 1), which showed the same trend as the initial/field enzyme activities. Within the first 50 cm, NAG and AP activity averaged 16.8 ± 1.60 nmol MUF g^{-1} min^{-1} and 10.5 ± 0.47 nmol MUF g^{-1} min^{-1}, respectively. From 50 to 100 cm, activity of NAG increased to an average of 36.1 ± 1.04 nmol MUF g^{-1} min^{-1}, while AP activity averaged 27.0 ± 0.74 nmol MUF g^{-1} min^{-1}. β-Glucosidase activity ranged from 15.7 ± 2.05 nmol MUF g^{-1} min^{-1} at 90–100 cm to 41.6 ± 4.03 nmol MUF g^{-1} min^{-1} at 70–80 cm. Activity of XY was lowest at 5–10 cm, where activity averaged 3.45 ± 0.81 nmol MUF g^{-1} min^{-1}, and greatest at 50–60 cm, where activity averaged 12.9 ± 2.65 nmol MUF g^{-1} min^{-1}. CB activity ranged from 9.88 ± 1.73 nmol MUF g^{-1} min^{-1} at 60–70 cm to 3.64 ± 0.62 nmol MUF g^{-1} min^{-1} at 40–50 cm. Activity of BG, XY, and CB were significant with site (Table 1). Both XY and CB activity were greatest at site 2, while BG activity was highest within site 3.

3.2.3. Microbial biomass C

Microbial biomass C was not significantly affected by treatment, but was affected by both depth and site (Table 1). Within site 3, MBC was greatest, averaging 15,952 ± 1513 mg kg^{-1}, though not significantly different from site 2. Similar to enzyme activity, MBC concentrations

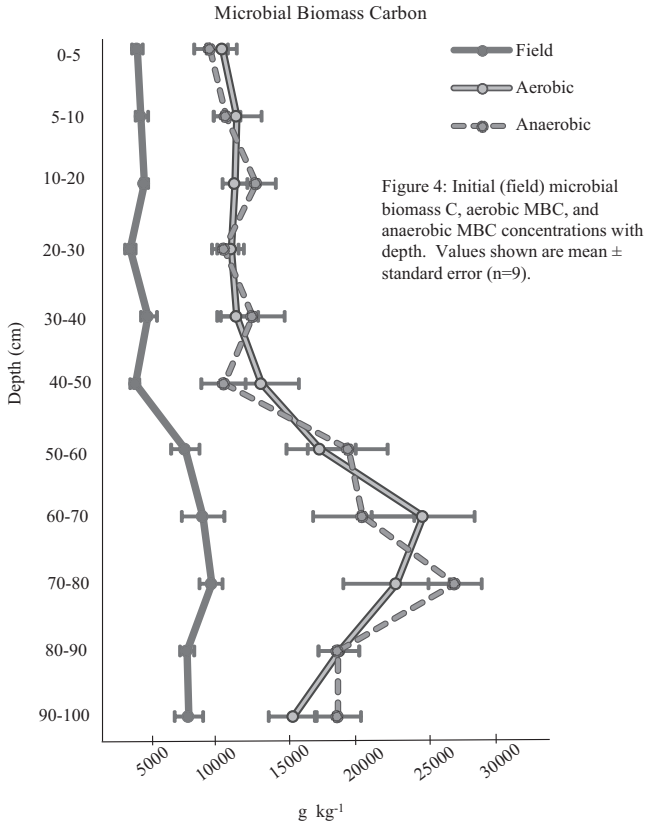

Figure 4: Initial (field) microbial biomass C, aerobic MBC, and anaerobic MBC concentrations with depth. Values shown are mean ± standard error (n=9).

Fig. 4. Initial (field) microbial biomass C, aerobic MBC, and anaerobic MBC concentrations with depth. Values shown are mean ± standard error (n = 9).

were lower between the surface (0–5 cm) and 50 cm, then increased roughly 2× from 50 to 100 cm.

3.2.4. Potentially mineralizable nutrients

Rates of potentially mineralizable NH_4^+ (PMN) were significantly different with the interaction between treatment and depth (Table 1). Within the aerobic treatment, the rates of PMN ranged from -0.03 ± 0.03 mg NH_4^+ d^{-1} at 30–40 cm to -1.31 ± 0.49 mg NH_4^+ d^{-1} at 0–5 cm. Negative rates of PMN indicate net immobilization of NH_4^+, rather than mineralization. Within the anaerobic treatment, PMN rates were positive from 0 to 40 cm, and negative from 50 cm to 100 cm (Fig. 7). Extractable SRP was generally below detection, and thus PMP rates could not be calculated.

4. Discussion

4.1. Field characteristics

Soil organic matter, total C, total N, and extractable DOC all exhibited the same trend, remaining relatively consistent from 0 to 50 cm, and then increasing at 50 cm (Fig. 2). Surprisingly, this trend is exhibited at all cores collected at all three sites, indicating that the increase in organic matter is not an isolated occurrence, but may be an artifact of the region's history. Barataria Bay is a highly dynamic area, impacted by both anthropogenic disturbances and high-energy storm events. Prior to the early 1900s, Barataria Bay was hydrologically connected to Bayou Lafourche, which supplied freshwater to the wetlands within the bay (Conner and Day, 1987; DeLaune and Lindau, 1987). A study by DeLaune (1986) examining C isotopes present within the soil to a depth of 130 cm indicated that the current brackish marshes of Barataria Bay were once freshwater marshes, exhibiting the low $\delta^{13}C$ values associated with freshwater marsh vegetation. The hydrologic isolation of Barataria Bay from the freshwater inputs of Bayou Lafourche in 1904 altered the salinity regime of these sites, causing the

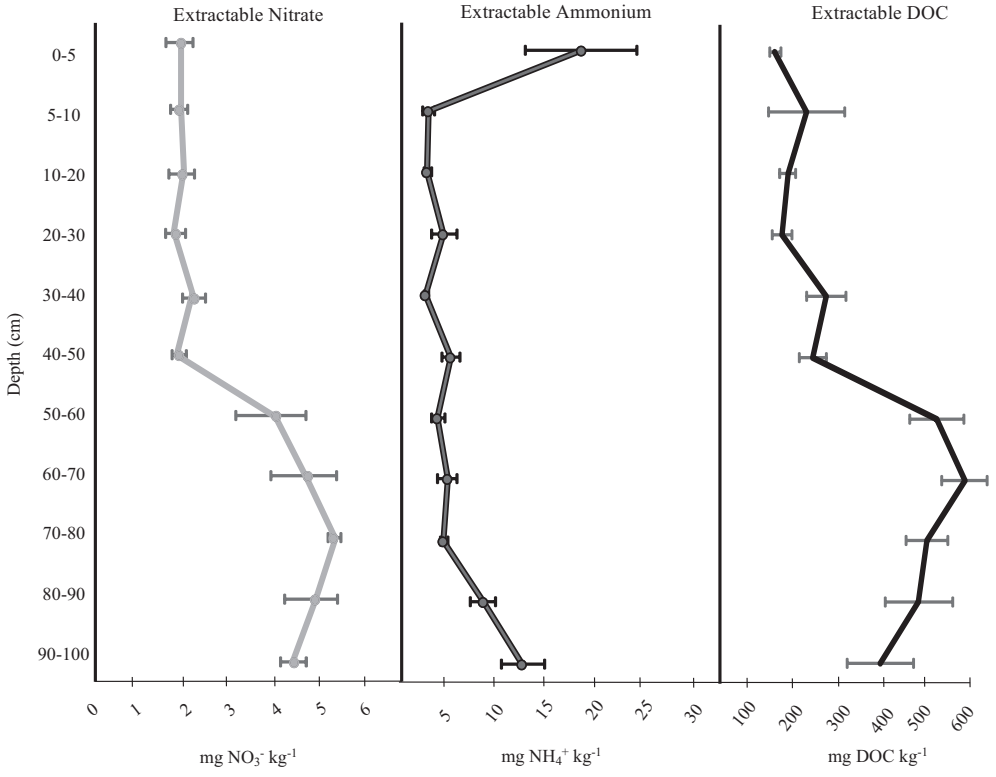

Fig. 5. Initial (field) extractable nitrate, extractable ammonium, and extractable DOC concentrations with depth. Values shown are mean ± standard error (n = 9).

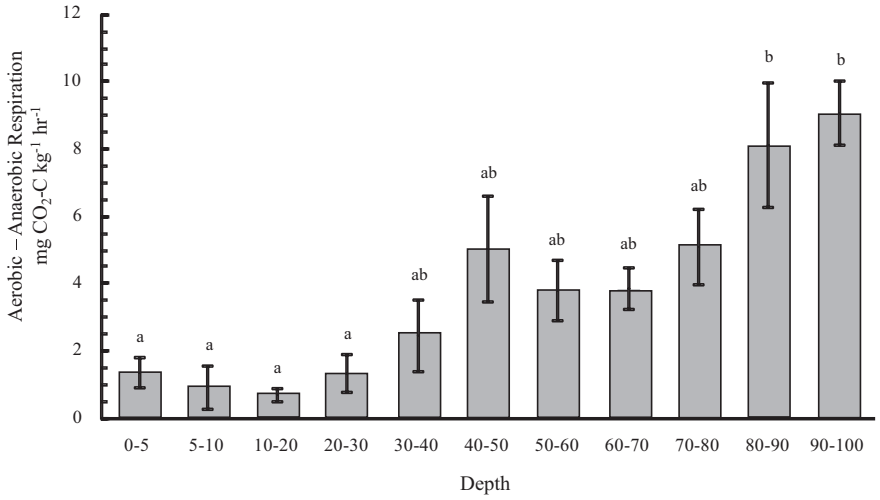

Fig. 6. Difference in respiration between aerobic treatments and anaerobic treatments by depth. Values shown are mean ± standard error (n = 9). Letters indicate significant differences between depths ($p < 0.05$).

marshes to become brackish (Conner and Day, 1987). The C-rich soil was then buried under a thin layer of mineral sediment, and brackish vegetation colonized the sites, leading to the deposition of less organic C into the soil matrix, likely associated with a greater tidal influence (Delaune, 1986; Reddy and DeLaune, 2008). Total phosphorus does not reflect this trend, and instead exhibits relatively stable concentrations with depth. Unlike C and N, the P cycle is tightly coupled to sorption and desorption with mineral components, flocculation and dissolution, leaching, and uptake by macrophytes, any of which could influence total P concentrations with depth (Reddy et al., 1999).

Similarly, depth significantly impacted all measured parameters of soil microbial activity (Figs. 3 and 4). It is generally accepted that the maximum amount of soil microbial activity occurs in the surficial soils (0–10 cm) or within the rhizophere of wetlands (Brix, 1987; Reddy et al., 1989). These hot spots of microbial activity are facilitated by oxygen diffusion into the soil matrix from the atmosphere or water column, as well as oxygen leaking out of the roots of wetland macrophytes to create a 2–3 mm thick oxidized rhizosphere (Brix, 1987; Reddy and DeLaune, 2008). However, in this study, the most microbially-active soil depths in the field were between 50 and 100 cm, substantially deeper than expected. Microbial biomass C increased nearly 50% between the 0–5 cm and 50–60 cm depths; NAG and BG enzyme activity and CO_2 production mirrored this increase, indicating that microbial activity can be greater at these depths than has been

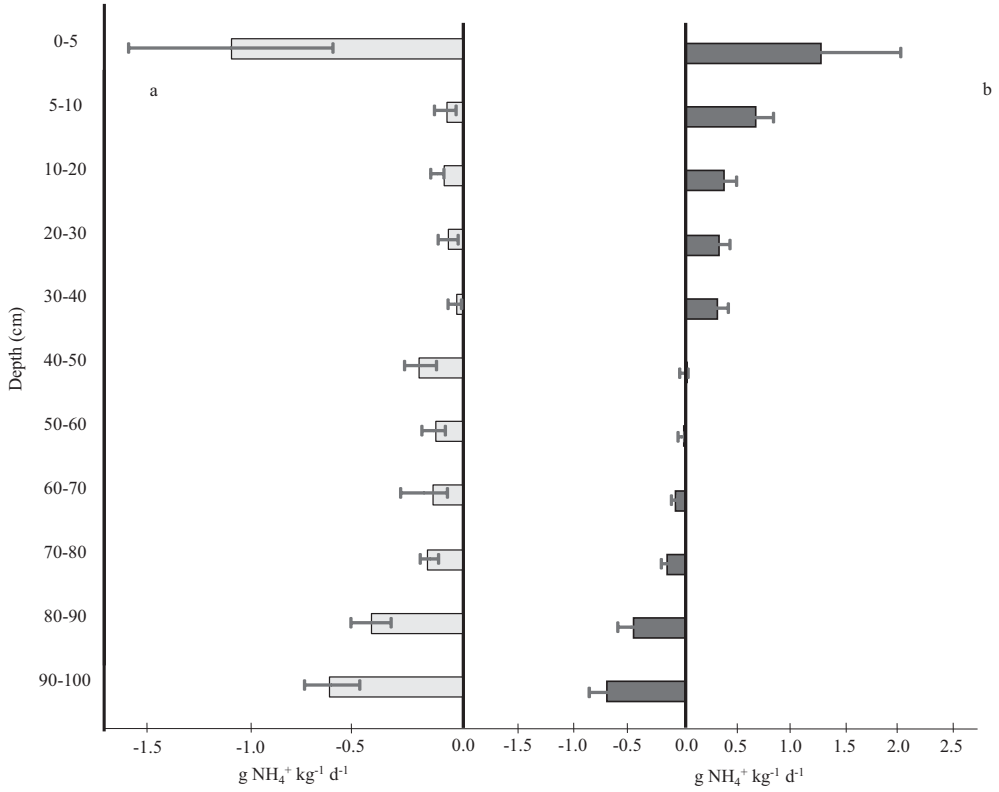

Fig. 7. Rates of potential aerobic ammonium (a) and anaerobic ammonium (b) mineralization with depth. Negative rates indicate immobilization, while positive rates indicate mineralization. Values shown are mean ± standard error (n = 9).

previously documented (Blume et al., 2002; Fierer et al., 2003). The increase microbial activity at depth is likely related to both the greater quality and quantity of organic matter and associated nutrients at depth. Activity of BG at these sites was roughly 3× greater than activity reported in a similar soil at a depth of 0–5 cm (Chambers et al., 2016). However, due to the small number of studies that have quantified rates of enzyme activity in brackish marsh soils, it is difficult to compare our rates to other systems.

Despite the abundance of organic matter found at depth in this study, anaerobic respiration in deep soils is typically limited by the availability of alternate electron acceptors, such as NO_3^- (Reddy and DeLaune, 2008; Fig. 7). Generally, NO_3^- present at depth within brackish wetlands is consumed preferentially over sulfate and lost via denitrification, the microbially-mediated anaerobic reduction of nitrogenous oxides to nitrogen gas (Tiedje, 1982). Denitrification rates within the brackish marsh of Barataria range from 44.6 to 2158 μmol $m^{-2} d^{-1}$ (Smith and De Laune, 1983), and more specifically, the denitrification rate at one of the sampling locations was 9.3 ± 0.3 mg N_2O-N $kg^{-1} h^{-1}$ (Pietroski et al., 2015). Though these rates would support a high removal of NO_3^-, measured extractable NO_3^- concentrations peaked between 50 and 100 cm at all three sites, indicating that nitrate is not being denitrified by the resident microbiota. Extractable nitrate values ranged from 0.79–1.25 mg/L between 50 and 100 cm, roughly half the concentration within the Mississippi River during spring floods (Turner and Rabalais, 1991). The presence of NO_3^-, combined with high rates of microbial activity, could indicate subsurface tidal flushing at these depths. Horizontal subsurface flow of seawater through the marsh platform has been observed within tidal marshes, and is often aerobic, contributing to the oxidation of iron within the soil matrix (Harvey et al., 1987; Huettel et al., 1998; Mann and Wetzel, 1995; Osgood, 2000; Taillefert et al., 2007). Subsurface flushing of seawater close to the marsh edge (1 m inland) could catalyze increases in CO_2 production, decreases in denitrification rates, and promote the mineralization of bioavailable N and P. Moreover, subsurface tidal flushing may also destabilize the marsh platform, accelerating marsh collapse and submergence.

4.2. CO_2 production

Oxygen is an electron acceptor thermodynamically favored over all other pathways of microbial respiration. As such, the addition of oxygen to soil microcosms increased CO_2 production at all depths within all sites, relative to the anaerobic treatment. However, the difference in respiration between treatments at the 90–100 cm depth was roughly 4× greater than respiration at the soil surface (Fig. 6), indicating exposure to O_2 accelerated soil respiration in deep soils to a much greater extent than in shallow soils. Though the chemical structure of present C was not directly measured, CO_2 production within both treatments increased at depth, indicating that the available soil C was readily decomposable, regardless of oxygen availability. Similar to MBC and enzyme activity, CO_2 production may be influenced by the site history and the availability of organic matter. Taking into account soil density, the differences in potential CO_2 production rate between the surface and deeper depths becomes more striking: 8.86 μg of CO_2-C $cm^{-3} h^{-1}$ is potentially lost within the 0–5 cm depth interval, while 95.1 μg of CO_2-C $cm^{-3} h^{-1}$ could be lost within 90–100 cm, a 10× difference in CO_2 loss. This disparity is due to the greater density of total C present deeper within the soil profile.

4.3. Nitrogen and phosphorus mineralization rates

An increase in respiration from an influx of oxygenated seawater can potentially mineralize inorganic forms of N and P during the degradation of organic compounds. Within the aerobic treatment, all potentially mineralized NH_4^+ was converted to NO_3^-, likely through nitrification, an oxidative process. From the soil surface to 50 cm, net mineralization of NH_4^+ was positive within the anaerobic treatment, though the magnitude decreased with depth, indicating that NH_4^+ is being released with respiration (Fig. 7). Immobilization, the transformation of inorganic forms of N to organic forms, was the dominant process deeper than 50 cm. Net immobilization suggests that the present N was being assimilated into the microbial biomass, which increased simultaneously to support increased decomposition of available C (Fig. 4). Owing to the observed increase in CO_2 production with depth in both treatments, we expected to see a concurrent release of nutrients (McLatchey and Reddy, 1998). The net N immobilization observed may be an artifact of the experimental design, as increasing microbial biomass C during the incubation period greatly enhanced the demand for inorganic N. Potentially mineralizable P was also quantified, but SRP concentrations were generally below detection.

4.4. Site history

Variable content of soil organic matter with depth was strongly correlated with measurements of microbial activity in this study, suggesting that site history (e.g., shifts in plant litter quality and quantity, hydrology, and depositional patterns over time) impacted current ecosystem functioning. These currently brackish marshes developed above previously existing freshwater marshes through the processes of burial and accretion with time, driven by shifts in inundation and salinity regimes (Delaune, 1986). The dynamic temporal nature of coastal ecosystems and plant communities has been documented by others, which have similarly observed different soil types and plant communities with depth (Brinson et al., 2018; Hussein, 2009; Mackie et al., 2005). These shifts in dominant vegetation preserved within the coastal wetland soils continue to occur as a result of sea level rise and climatic change (e.g., mangrove encroachment into salt marshes; Kelleway et al., 2017), and can be further accelerated by anthropogenic hydrologic modifications, such as levees and freshwater diversions (Delaune, 1986; Nyman et al., 1990). Therefore, although the results of this study are specific to this region's unique site history of hydrologic isolation, similar patterns of shifting organic matter content and quality with depth can be expected in many coastal wetlands, underlining the need to sample deeper into the soil profile to fully understand the consequences of wetland erosion and submergence on stored C and nutrients.

5. Conclusions

In organogenic wetlands, submergence induced by sea level rise endangers the large stocks of C sequestered within coastal soil. Though the general paradigm within wetland science is that the degradability of soil organic matter decreases with depth (Gale and Gilmour, 1988; Maltby, 1988; Mendelssohn et al., 1999; Schipper and Reddy, 1995; Schipper et al., 2002; Webster and Benfield, 1986), this study challenges that assumption: increases in enzyme activity, microbial biomass C, and CO_2 production at depth indicates the sequestered C is not particularly recalcitrant (Reddy and DeLaune, 2008; Stevenson and Cole, 1999). Our findings indicate these deeper (> 50 cm) organic matter stocks can be vulnerable to mineralization, especially following wetland erosion and submergence. More specifically, aerobic conditions, which could be stimulated by the availability of dissolved oxygen within seawater, can increase CO_2 production by 66% relative to the anaerobic conditions that typically pervade in an intact marsh. This potential increase in mineralization results in a loss of organic C within the soil matrix, increasing global warming potential of these marshes. For example, if just 25% of the organic C present within 1 m of the soil profile is mineralized due to submergence and mixing with oxygenated seawater, we can expect approximately 8472–11,866 Gg of C released to the atmosphere annually from this region of coastal LA, based on the mass of C present in these soils.

Additionally, this study highlights the need to collect and study

deeper soil cores within dynamic coastal wetland environments. Often, soil cores are collected to shallower depths (i.e., 20 or 30 cm; Gardner and White, 2010; Levine et al., 2017; Marton and Roberts, 2014), owing to the assumption that most microbial activity happens at the surface (Reddy and DeLaune, 2008). However, many coastal wetland systems have undergone decades of change, including shifts in vegetation communities and deposition patterns, requiring deeper sampling and an understanding of site history to fully determine the implications of submergence on the global C cycle.

Acknowledgements

The authors thank Benjamin Haywood, Michael Patrick Hayes, and Amanda Fontenot for field assistance, Drs. Robert Cook and George Xue for guidance, and Nia Hurst for assistance with sample analysis. This work was funded under a collaborative National Science Foundation Chemical Oceanography Grant (#1635837).

References

Amthor, J.S., Huston, M.A., 1998. Terrestrial Ecosystem Responses to Global Change: A Research Strategy. ORNL Oak Ridge National Laboratory, US.

Andersen, J.M., 1976. An ignition method for determination of total phosphorus in lake sediments. Water Res. 10 (4), 329–331.

Baumann, R.H., Day, J.W.J., Miller, C.A., 1984. Mississippi deltaic wetland survival - sedimentation versus coastal submergence. Science 80 (224), 1093–1095.

Bianchi, T.S., Canuel, E.A., 2011. Chemical biomarkers in aquatic ecosystems. Princeton University Press.

Bianchi, T.S., Dimarco, S.F., Allison, M.A., Chapman, P., Cowan, J.H., Hetland, R.D., Morse, J.W., Rowe, G., 2008. Controlling hypoxia on the U.S. Louisiana Shelf: beyond the nutrient-centric view. EOS Trans. Am. Geophys. Union 89, 236–237. https://doi.org/10.1029/2008EO260005.

Blume, E., Bischoff, M., Reichert, J.M., Moorman, T., Konopka, A., Turco, R.F., 2002. Surface and subsurface microbial biomass, community structure and metabolic activity as a function of soil depth and season. Appl. Soil Ecol. 20, 171–181.

Bridgham, S.D., Updegraff, K., Pastor, J., 1998. Carbon, nitrogen, and phosphorus mineralization in northern wetlands. Ecology 79, 1545–1561.

Brinson, M.M., Christian, R.R., Blum, L.K., Estuaries, S., Odum, W.E., Symposium, M., Blum, L.K., 2018. Multiple States in the Sea-level Induced Transition from Terrestrial Forest to Estuary Linked References Are Available on JSTOR for This Article: Multiple States in the Sea-level Induced Transition From Terrestrial. 18. pp. 648–659.

Brix, H., 1987. Treatment of wastewater in the rhizosphere of wetland plants–the root-zone method. Water Sci. Technol. 19, 107–118.

Chambers, L.G., et al., 2016. Effects of salinity and inundation on microbial community structure and function in a mangrove peat soil. Wetlands 36 (2), 361–371.

Church, J.A., Clark, P.U., Cazenave, A., Gregory, J.M., Jevrejeva, S., Levermann, A., Merrifield, M.A., Milne, G.A., Nerem, R.S., Nunn, P.D., 2013. Sea Level Change (PM). Cambridge University Press.

Conner, W., Day, J.W., 1987. The Ecology of Barataria Basin, Louisiana: An Estuarine Profile.

DeBusk, W.F., Reddy, K.R., 1998. Turnover of detrital organic carbon in a nutrient-impacted Everglades marsh. Soil Sci. Soc. Am. J. 62, 1460–1468.

Delaune, R.D., 1986. The Use of 613C Signature of C-3 and C-4 Plants in Determining Past Depositional Environments in Rapidly Accreting Marshes of the Mississippi River. 59. pp. 315–320.

DeLaune, R.D., Lindau, C.W., 1987. δ13C signature of organic carbon in estuarine bottom sediment as an indicator of carbon export from adjacent marshes. Biogeochemistry 4, 225–230. https://doi.org/10.1007/BF02187368.

DeLaune, R.D., Pezeshki, S.R., 2003. The role of soil organic carbon in maintaining surface elevation in rapidly subsiding US Gulf of Mexico coastal marshes. Water Air Soil Pollut. Focus 3, 167–179.

DeLaune, R.D., White, J.R., 2012. Will coastal wetlands continue to sequester carbon in response to an increase in global sea level? A case study of the rapidly subsiding Mississippi river deltaic plain. Clim. Chang. 110, 297–314. https://doi.org/10.1007/s10584-011-0089-6.

Delaune, R.D., Reddy, C.N., Patrick, W.H., 1981. Accumulation of Plant Nutrients and Heavy Metals Through Sedimentation Processes and Accretion in a Louisiana Salt Marsh. 4. pp. 328–334.

Eldridge, P.M., Morse, J.W., 2008. Origins and temporal scales of hypoxia on the Louisiana shelf: Importance of benthic and sub-pycnocline water metabolism. Mar. Chem. 108 (3-4), 159–171.

Fierer, N., Schimel, J.P., Holden, P.A., 2003. Variations in microbial community composition through two soil depth profiles. Soil Biol. Biochem. 35, 167–176.

Gale, P.M., Gilmour, J.T., 1988. Net mineralization of carbon and nitrogen under aerobic and anaerobic conditions. Soil Sci. Soc. Am. J. 52, 1006–1010. https://doi.org/10.2136/sssaj1988.03615995005200040019x.

Gardner, L.M., White, J.R., 2010. Denitrification enzyme activity as an indicator of nitrate movement through a diversion wetland. Soil Sci. Soc. Am. J. 74, 1037–1047.

German, D.P., Weintraub, M.N., Grandy, A.S., Lauber, C.L., Rinkes, Z.L., Allison, S.D., 2011. Optimization of hydrolytic and oxidative enzyme methods for ecosystem studies. Soil Biol. Biochem. 43, 1387–1397. https://doi.org/10.1016/j.soilbio.2011.03.017.

Harvey, J.W., Germann, P.F., Odum, W.E., 1987. Geomorphological control of subsurface hydrology in the creekbank zone of tidal marshes. Estuar. Coast. Shelf Sci. 25, 677–691. https://doi.org/10.1016/0272-7714(87)90015-1.

Hatton, R.S., Delaune, R.D., Patrick, W.H.J., 1983. Sedimentation, accretion, and subsidence in marshes of Barataria Basin, Louisiana. Limnol. Oceanogr. 28, 494–502. https://doi.org/10.4319/lo.1983.28.3.0494.

Huettel, M., Ziebis, W., Forster, S., Luther, G.W., 1998. Advective transport affecting metal and nutrient distributions and interfacial fluxes in permeable sediments. Geochim. Cosmochim. Acta 62, 613–631. https://doi.org/10.1016/S0016-7037(97)00371-2.

Hussein, A.H., 2009. Modeling of sea-level rise and deforestation in submerging coastal ultisols of Chesapeake Bay. Soil Sci. Soc. Am. J. 73, 185–196. https://doi.org/10.2136/sssaj2006.0436.

IPCC, 2014. Climate Change 2014: Synthesis Report. Contribution of Working Groups I, II and III to the Fifth Assessment Report of the Intergovernmental Panel on Climate Change. In: Core Writing Team, Pachauri, R.K., Meyer, L.A. (Eds.), IPCC, Geneva, Switzerland (151 pp.).

Kelleway, J.J., Cavanaugh, K., Rogers, K., Feller, I.C., Ens, E., Doughty, C., Saintilan, N., 2017. Review of the ecosystem service implications of mangrove encroachment into salt marshes. Glob. Chang. Biol. 23, 3967–3983. https://doi.org/10.1111/gcb.13727.

Kirwan, M.L., Megonigal, J.P., 2013. Tidal wetland stability in the face of human impacts and sea-level rise. Nature 504, 53.

Levine, B.M., White, J.R., DeLaune, R.D., 2017. Impacts of the long-term presence of buried crude oil on salt marsh soil denitrification in Barataria Bay, Louisiana. Ecol. Eng. 99, 454–461.

Mackie, E.A.V., Leng, M.J., Lloyd, J.M., Arrowsmith, C., 2005. Bulk organic δ13C and C/N ratios as palaeosalinity indicators within a Scottish isolation basin. J. Quat. Sci. 20, 303–312. https://doi.org/10.1002/jqs.919.

Maltby, E., 1988. Cotton strip assay: an index of decomposition in. Soils 129–130.

Mann, C.J., Wetzel, R.G., 1995. Dissolved organic carbon and its utilization in a riverine wetland ecosystem. Biogeochemistry 31, 99–120.

Marton, J.M., Roberts, B.J., 2014. Spatial variability of phosphorus sorption dynamics in Louisiana salt marshes. J. Geophys. Res. Biogeosci. 119, 451–465.

McLatchey, G.P., Reddy, K.R., 1998. Regulation of organic matter decomposition and nutrient release in a wetland soil. J. Environ. Qual. https://doi.org/10.2134/jeq1998.00472425002700050036x.

Melillo, J.M., Aber, J.D., Linkins, A.E., Ricca, A., Fry, B., Nadelhoffer, K.J., 1989. Carbon and nitrogen dynamics along the decay continuum: plant litter to soil organic matter. Plant Soil 115, 189–198.

Mendelssohn, I.A., Sorrell, B.K., Brix, H., Schierup, H.H., Lorenzen, B., Maltby, E., 1999. Controls on soil cellulose decomposition along a salinity gradient in a *Phragmites australis* wetland in Denmark. Aquat. Bot. 64, 381–398. https://doi.org/10.1016/S0304-3770(99)00065-0.

Nyman, J.A.A., Delaune, R.D.D., Patrick, W.H.H., 1990. Wetland soil formation in the rapidly subsiding Mississippi River Deltaic Plain - mineral and organic-matter relationships. Estuar. Coast. Shelf Sci. 31, 57–69. https://doi.org/10.1016/0272-7714(90)90028-P.

Odum, E.P., 1968. Energy flow in ecosystems: a historical review. Am. Zool. 8, 11–18.

Osgood, D.T., 2000. Subsurface hydrology and nutrient export from barrier island marshes at different tidal ranges. Wetl. Ecol. Manag. 8, 133–146. https://doi.org/10.1023/A:1008488317880.

Ouyang, X., Lee, S.Y., 2014. Updated estimates of carbon accumulation rates in coastal marsh sediments. Biogeosciences 11, 5057–5071. https://doi.org/10.5194/bg-11-5057-2014.

Penland, S., Wayne, L., Britsch, D., Williams, S.J., Beall, A.D., Butterworth, V., 2000. Process Classification of Coastal Land Loss Between 1932 and 1990 in the Mississippi River Delta Plain, Southeastern Louisiana. 1 USGS.

Pietroski, J.P., White, J.R., DeLaune, R.D., Wang, J.J., Dodla, S.K., 2015. Fresh and weathered crude oil effects on potential denitrification rates of coastal marsh soil. Chemosphere 134, 120–126.

Rakocinski, C.F., Baltz, D.M., Fleeger, J.W., 1992. Correspondence between environmental gradients and the community structure of marsh-edge fishes in a Louisiana estuary. Mar. Ecol. Prog. Ser. 135–148.

Reddy, K.R., DeLaune, R.D., 2008. Biogeochemistry of Wetlands: Science and Applications. CRC Press.

Reddy, K.R., Patrick, W.H., Lindau, C.W., 1989. Nitrification-denitrification at the plant root-sediment interface in wetlands. Limnol. Oceanogr. 34, 1004–1013.

Reddy, K.R., Kadlec, R.H., Flaig, E., Gale, P.M., 1999. Phosphorus retention in streams and wetlands: a review. Crit. Rev. Environ. Sci. Technol. 29, 83–146. https://doi.org/10.1080/10643389991259182.

RStudio Team, 2015. RStudio: Integrated Development for R. RStudio, Inc., Boston, MA. http://www.rstudio.com/.

Schipper, L.A., Reddy, K.R., 1995. In situ determination of detrital breakdown in wetland soil-floodwater profile. Soil Sci. Soc. Am. J. 1437, 565–568. https://doi.org/10.1126/science.1146511.

Schipper, L. a, Mcleod, M., Scott, N., Clarkson, B., Smith, J., Campbell, D., 2002. Subsidence rates and carbon loss in peat soils following conversion to pasture in the Waikato Region, New Zealand. Soil Use Manag. 18, 91–93. https://doi.org/10.1079/SUM2001106.

Smith, C.J., De Laune, R.D., 1983. Nitrogen loss from freshwater and saline estuarine sediments. J. Environ. Qual. 12, 514–518.

Stevenson, F.J., Cole, M.A., 1999. Cycles of Soils: Carbon, Nitrogen, Phosphorus, Sulfur, Micronutrients. John Wiley & Sons.

Taillefert, M., Neuhuber, S., Bristow, G., 2007. The effect of tidal forcing on

biogeochemical processes in intertidal salt marsh sediments. Geochem. Trans. 8, 6.
Tiedje, J.M., 1982. Denitrification. In: Methods Soil Anal. Part 2. Chem. Microbiol. Prop, pp. 1011–1026.
Turner, R.E., Rabalais, N.N., 1991. Changes in Mississippi River water quality this century. Bioscience 41, 140–147.
Updegraff, K., Pastor, J., Bridgham, S.D., Johnston, C.A., 1995. Environmental and substrate controls over carbon and nitrogen mineralization in northern wetlands. Ecol. Appl. 5, 151–163.
U.S. Geological Survey, 2018. National Water Information System data available on the World Wide Web (USGS Water Data for the Nation).
Vance, E.D., Brookes, P.C., Jenkinson, D.S., 1987. An extraction method for measuring soil microbial biomass C. Soil Biol. Biochem. 19, 703–707.
Webster, J.R., Benfield, E.F., 1986. Vascular plant breakdown in freshwater ecosystems. Annu. Rev. Ecol. Syst. 17, 567–594.
White, J.R., DeLaune, R.D., Li, C.Y., Bentley, S.J., 2009. Sediment methyl and total mercury concentrations along the Georgia and Louisiana Inner Shelf, USA. Anal. Lett. 42, 1219–1231. https://doi.org/10.1080/00032710902901947.